



Article scientifique

Article

1999

Published version

Open Access

This is the published version of the publication, made available in accordance with the publisher's policy.

Purification and analysis of authentic CLIP-170 and recombinant fragments

Scheel, Jochen Konrad; Pierre, Philippe; Rickard, Janet Elizabeth; Diamantopoulos, Georgios; Valetti, Caterina; Van Der Goot Grunberg, Françoise G.; Häner, Markus; Aebi, Ueli; Kreis, Thomas

How to cite

SCHEEL, Jochen Konrad et al. Purification and analysis of authentic CLIP-170 and recombinant fragments. In: The Journal of biological chemistry, 1999, vol. 274, n° 36, p. 25883–25891. doi: 10.1074/jbc.274.36.25883

This publication URL: <https://archive-ouverte.unige.ch/unige:166719>

Publication DOI: [10.1074/jbc.274.36.25883](https://doi.org/10.1074/jbc.274.36.25883)

© The author(s). This work is licensed under a Creative Commons Attribution (CC BY)

<https://creativecommons.org/licenses/by/4.0>

Purification and Analysis of Authentic CLIP-170 and Recombinant Fragments*

(Received for publication, March 30, 1999, and in revised form, June 14, 1999)

Jochen Scheel,^{a,b,c} Philippe Pierre,^{a,c,d} Janet E. Rickard,^{a,c,e} Georgios S. Diamantopoulos,^a Caterina Valetti,^{a,f} F. Gisou van der Goot,^g Markus Häner,^h Ueli Aebi,^h and Thomas E. Kreis^{a,i}

From the ^aDepartment of Cell Biology, Sciences III, and ^gDepartment of Biochemistry, Sciences II, University of Geneva, CH-1211 Geneva 4 and ^hBiozentrum, M. E. Müller Institute for Structural Biology, University of Basel, CH-4056 Basel, Switzerland

We have purified authentic CLIP-170 (cytoplasmic linker protein of 170 kDa) and fragments comprising functional domains of the protein to characterize the structural basis of the function of CLIP-170. Analysis of authentic CLIP-170 and the recombinant fragments by electron microscopy after glycerol spraying/low angle rotary metal shadowing reveals CLIP-170 as a thin, 135-nm-long molecule with two kinks in its central rod domain, which are approximately equally spaced from the two ends of the protein. The central domain consisting of heptad repeats, which is α -helical in nature and forms a 2-stranded coiled-coil, mediates dimerization of CLIP-170. The rod domain harbors two kinks, each spaced \sim 37 nm from the corresponding end of the molecule, thus providing mechanical flexibility to the highly elongated molecule. The N-terminal domain of CLIP-170 binds to microtubules *in vitro* with a stoichiometry of one dimeric head domain per four tubulin heterodimers. Authentic CLIP-170 binds to microtubules with lower stoichiometry, indicating that the rod and tail domains affect microtubule binding of CLIP-170. These results document that CLIP-170 is a highly elongated polar molecule with the microtubule-binding domain and the organelle-interacting domains at opposite ends of the homodimer, thus providing a structural basis for the function of CLIP-170 as a microtubule-organelle linker protein.

in Ref. 2), as well as being dependent on force-generating proteins (reviewed in Ref. 3). Accessory proteins in addition to motor proteins like kinesins or dyneins are required to regulate and specify organelle-microtubule interactions (4, 5). CLIP-170 (6) is a non-motor MBP originally identified in HeLa cells (7), which localizes preferentially to elongating microtubule plus ends (8, 9) and is proposed to mediate interactions of endocytotic organelles (10) and chromosomes (11) with microtubules. The primary structure of CLIP-170 predicts a protein that is elongated, with two functional domains separated by a 950-amino acid stretch of heptad repeats. The N-terminal domain has two conserved motifs shown to mediate binding of the protein to microtubules (10). The C-terminal domain, on the other hand, is predicted to interact with other organelles and has been shown to mediate targeting of CLIP-170 to prometaphase kinetochores (11). The C-terminal domain, which contains two predicted metal-binding motifs, and the N-terminal microtubule-binding domains are highly conserved in vertebrate CLIP-170 homologues (10, 12) and in the putative *Drosophila melanogaster* CLIP-170 homologue, D-CLIP-190 (13), suggesting they play an important functional role.

The microtubule-binding domain of CLIP-170 (10) shows similarities to dp150^{glued} (14, 15), a subunit of the dynein complex, which is involved in regulating cytoplasmic dynein activity (reviewed in Ref. 4). In contrast to dp150^{glued}, however, CLIP-170 is not part of a protein complex. Bik1p, which is required for microtubule-related functions during mitosis in yeast, also contains a microtubule-binding domain similar to CLIP-170 (16), as do two proteins implicated in correct folding of α - and β -tubulin (17, 18). This motif, therefore, appears in several proteins with distinct roles in microtubule function (reviewed in Ref. 6). One of the C-terminal metal-binding motifs is also found in the yeast protein Bik1p (16). Dp150^{glued} and Bikp have an additional similarity to CLIP-170 in that they contain predicted heptad repeats that should allow dimerization, although this has not been established experimentally. Thus, the sequence of CLIP-170 predicts three major domains, each of which shows homology with domains in related proteins and are predicted to play specific functional roles.

Further analysis of the structure and activity of CLIP-170 is necessary to understand its *in vivo* function. For this purpose, highly purified protein as well as fragments comprising functional domains are required. We have developed a protocol for purification of authentic CLIP-170 from human placenta based on immunoaffinity chromatography (19), and we have also used the cDNA from HeLa cells (10) to express and purify predicted

Correct intracellular membrane traffic and the cytoarchitecture of eukaryotic cells depends on cytoplasmic microtubules. The dynamic properties intrinsic to tubulin assembly could also be regulated by interactions of cell organelles with microtubules (1). These interactions are mediated by MBPs¹ (reviewed

* This work was supported by the Swiss National Science Foundation (to T. E. K., J. E. R., F. G. v. d. G., and U. A.), the Canton de Genève (to T. E. K.), the M. E. Müller Foundation of Switzerland (to U. A.), and the Canton Basel-Stadt (to M. H.). The costs of publication of this article were defrayed in part by the payment of page charges. This article must therefore be hereby marked "advertisement" in accordance with 18 U.S.C. Section 1734 solely to indicate this fact.

^b Present address: Artemis Pharmaceuticals GmbH, Tübingen, Germany.

^c These authors contributed equally to this work.

^d Present address: Dept. of Cell Biology, Yale University School of Medicine, New Haven, CT.

^e Present address and to whom correspondence should be addressed: Dept. of Mental Health, University of Aberdeen Medical School, Foresterhill, Aberdeen, AB25 2ZD, Scotland. Tel.: 0044 1224 273101; Fax: 0044 1224 849191; E-mail: j.rickard@abdn.ac.uk.

^f Present address: Dept. of Experimental Medicine, University of Genova, Genova, Italy.

ⁱ Deceased.

¹ The abbreviations used are: MBP, microtubule-binding protein;

CLIP, cytoplasmic linker protein; mAb, monoclonal antibody; MAP, microtubule-associated protein; PAGE, polyacrylamide gel electrophoresis; PCR, polymerase chain reaction; PIPES, 1,4-piperazine-diethanesulfonic acid.

TABLE I
Purification table for isolation of CLIP-170 from human placenta

	Volume	Total protein		CLIP-170 content ^a		Enrichment		Yield	
		ml	mg/ml	mg	Total	per mg protein	cf, previous fraction	Total	From previous fraction
High speed supernatant	900	56	50,400	30	0.006	1	1	100	100
Antibody column	30	0.2	6.0	21	3.5	5800	5800	70	70
Microtubule affinity	0.3	1.0	0.3	7	23	6.6	38000	33	23
Superose 12	0.5	0.4	0.2	5	25	1.1	42000	71	16

^a Concentrations of CLIP-170 were measured by densitometric analysis of immunoblots, using dilution series of samples from each stage of purification, and are expressed as arbitrary units (25 units = 1 mg of purified CLIP-170). The concentration of CLIP-170 in placenta high speed supernatant was found to be 1.3 μ g/ml, corresponding to 0.002% of the total protein.

functional domains of the protein. A combination of biochemical, biophysical, and electron microscopy analyses reveals CLIP-170 as a highly elongated homodimer, with microtubule-binding and organelle-interacting domains separated by an α -helical 2-stranded coiled-coil domain. This rod domain, which contains two prominent kinks, and the C-terminal tail appear to negatively influence the binding of CLIP-170 to microtubules. These results provide a structural basis for the function of CLIP-170 as a microtubule-organelle linker protein.

EXPERIMENTAL PROCEDURES

Purification of CLIP-170—CLIP-170 was purified from human placenta by immunoaffinity chromatography and microtubule affinity as described (20). Proteins copurifying with CLIP-170 were not detected even when the 1 M salt wash step of the affinity column was omitted. CLIP-170 eluted from microtubules by high salt was either dialyzed against NMEG (50 mM NH_4OAc , 0.1 mM MgSO_4 , 0.5 mM EGTA, 20% glycerol, pH 6.9) or further purified by gel filtration chromatography using a Superose 12 column (Superose 12 HR 10/30; Amersham Pharmacia Biotech). 0.3-ml samples were loaded and separated at 0.5 ml/min in PEM (0.1 M KPIPES, 2 mM EGTA, 1 mM MgSO_4 , pH 6.8) or NMEG. Fractions of 0.2 ml were collected and analyzed by UV spectrophotometry and SDS-PAGE. Fractions containing pure CLIP-170 with more than 0.1 mg/ml protein were pooled and either analyzed directly or frozen in liquid nitrogen and stored at -80°C .

Generation of Recombinant CLIP-170 Fragments—An *NdeI* restriction site was introduced at the first ATG codon of the CLIP-170 cDNA in pBS KS by PCR mutagenesis to obtain plasmid pCLIP-*NdeI* (21). The head fragments were generated by first inserting an *NdeI*-*XhoI* fragment from this plasmid into pET19b (Novagen, AMS, Lugano, Switzerland), which allows expression with an N-terminal stretch of histidines, and then deleting parts of the rod and tail by digestions with *EspI* (H2) and religation, or with *KpnI*/*EspI* (H1) or *SphI*/*BamHI* (H3), blunting of the ends, and religation. All positions given are for the cDNA according to Pierre *et al.* (10). T1 was introduced in pET19b after digestion of the pCLIP-*NdeI* plasmid using a first *XhoI* (nucleotide 3860) site in the region coding for the C-terminal part of CLIP-170 and a second site in the vector. Tail domains (T2, T3, T4, T5, and T6) were amplified by the PCR on plasmid pM1CLIP-170 (10) using appropriate forward primers containing an *NdeI* site and a second primer in the 3'-nontranslated region of CLIP-170 cDNA incorporating an *EcoRV* site. PCR products were digested with *NdeI* and *EcoRV* and cloned into pET19b which had been digested with *NdeI* at the 3' end and *BamHI* followed by blunting with T4 polymerase at the 5' end. The rod domain was introduced in pET19b following a similar PCR-based strategy using an *NdeI* site at the 5' end and the *XhoI* site (position 3864) to eliminate the C-terminal domain of CLIP-170. The following primers were used: forward primers, R (primer position 1392) 5'-GCGACATATGGTGGGAAGCTGCTGA-3'; T6 (2184) 5'-TAAACATATGGAAGCCTTGAGGGCT-3'; T5 (2630) 5'-AGACATATGCAAGAAACTGTAAAT-3'; T4 (3054) 5'-AAGCATATG-GAAACAAGCCACAAC-3'; T3 (3320) 5'-AAGCATATGACTCTGGC-CTCCTTGGAG-3'; T2 (3557) 5'-AAACATATGGAGGAGCTGGGGAGA-3'; reverse primer (4300) 5'-CGTCTGAGCAAGCCCACT-3'.

All constructs were expressed in *Escherichia coli* strain BL21(DE3)pLysS except for T1 which was expressed in HMS174(DE3)pLysS (Novagen) by growth of well-aerated cultures at 37°C to OD <0.5 , induction of protein expression by addition of 1 mM isopropyl β -D-thiogalactopyranoside, and further incubation for 2.5 h at 37°C . Bacteria were harvested by centrifugation, washed in 0.2 volumes of 40 mM Tris-HCl, 10 mM imidazole, pH 8.0, resuspended in 0.05 volumes of the same buffer, and snap-frozen in liquid nitrogen. After freezing, the cells were left at least 5 min in liquid nitrogen

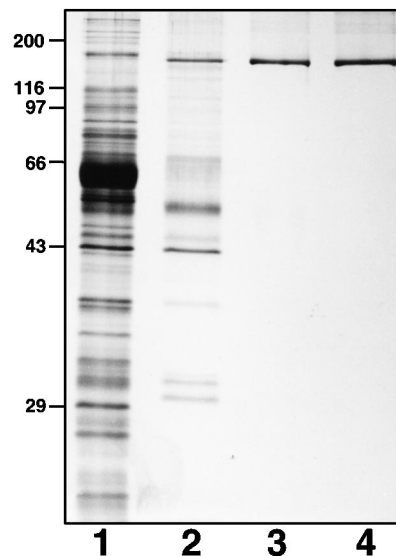


FIG. 1. SDS-PAGE analysis of CLIP-170 purification from human placenta. Samples of the high speed supernatant (lane 1), the eluate of the immunoaffinity column (lane 2), the microtubule eluate (lane 3), and the peak fractions eluted from the gel filtration column (lane 4) during the preparation of CLIP-170 were analyzed by 10% SDS-PAGE followed by silver staining. Molecular weights ($\times 10^{-3}$) are shown on the left.

or, more usually, overnight at -80°C before thawing quickly in a 37°C water bath. The thawed lysate was incubated with 25 μ g/ml DNase I, 5 mM MgCl_2 , and 0.2% Triton X-100 for 5–30 min at 0°C until no longer viscous. After addition of one sample volume of 1 M NaCl, the lysate was cleared by centrifugation at $25,000 \times g$ for 20 min at 4°C . Cleared lysates were used directly for immunoblotting or recombinant proteins were purified by metal chelate chromatography. For all constructs except T1, 1-ml columns of His-bind[®] resin (Novagen) charged with Ni^{2+} were equilibrated with 5 mM imidazole, 0.5 M NaCl, 20 mM Tris-HCl, pH 7.9, before loading cleared lysates derived from up to 250 ml of bacterial culture. Columns were washed with 5 column volumes of 60 mM imidazole, 0.5 M NaCl, 20 mM Tris-HCl, pH 7.9, before elution of bound proteins by 1 M imidazole, 0.5 M NaCl, 20 mM Tris-HCl, pH 7.9. For the T1 construct, protein purified by this method was found to be aggregated, so it was purified using nickel-nitrilotriacetic acid resin (Diagen GmbH, Düsseldorf, Germany) which allowed the use of reducing agent. The protocol was as above except that 10 mM 2-mercaptoethanol was included in the washing/freezing buffer and all the column buffers and 1 mM dithiothreitol was included in buffers for dialysis and individual experiments. Fractions of 0.5 ml were collected from the columns, and protein-containing fractions were pooled. Proteins were dialyzed into the buffers described for individual experiments and either used directly or snap-frozen in liquid nitrogen and stored at -80°C .

Epitope Mapping and Immunoblotting—Proteins from cleared lysates of isopropyl β -D-thiogalactopyranoside-induced clones harboring expression constructs of CLIP-170 were analyzed by immunoblotting as described (7) using monoclonal (19) and polyclonal (10) antibodies against CLIP-170. None of the mAbs 2D6, 3A3, and 4D3 bound to H fragments. mAb 2D6 bound to all the tail fragments including T1 but not to R, which places the epitope of mAb 2D6 beyond amino acid 1237. mAbs 3A3 and 4D3 bound to fragments T4, T5, and T6 and to R, but not to fragments T3, T2, or T1, which places the epitope of these two

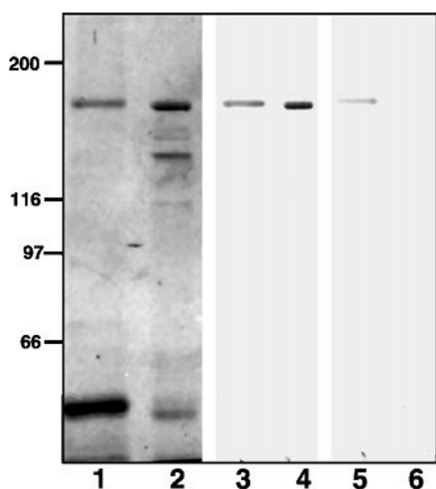


FIG. 2. Comparison of HeLa and placenta CLIP-170 by SDS-PAGE and immunoblotting with two anti-peptide antibodies. CLIP-170 purified by antibody affinity column from HeLa cells (lanes 1, 3 and 5) or human placenta (lanes 2, 4 and 6) was separated by 7% SDS-PAGE, and the gels were stained with Coomassie Blue (lanes 1 and 2) or immunoblotted with anti-KRKV (lanes 3 and 4) or anti-KMRL (lanes 5 and 6) anti-peptide antibodies. Numbers at the left indicate the position of molecular weight markers ($\times 10^{-3}$). CLIP-170 from HeLa cells or placenta have a very similar electrophoretic mobility, but of the two anti-peptide antibodies used here, both raised against sequences of the HeLa protein, only one reacts with the protein from placenta, indicating some sequence difference between the proteins from the two sources. Note that the anti-KRKV reactivity shows that slightly more placenta CLIP-170 than HeLa CLIP-170 was loaded on the gel, which means that the lack of reaction with the anti-KMRL antibody is not a problem of detection limit.

monoclonal antibodies between amino acids 971 and 1059. The polyclonal anti-55 antibody (10) bound fragments H2, H3, and R, but not H1; the main epitope of this antibody thus appears to be confined to the sequence between amino acid 350 and 854. The localization of these antibody epitopes is summarized in Fig. 4. The ability of 4D3 to bind to the rod domain but not the C-terminal domain allows the effect of cellular overexpression of the tail domain on localization of the endogenous protein to be studied (11).

Circular Dichroism and Amino Acid Analysis—Circular dichroic experiments were performed at room temperature using a Jasco 600 autodichrograph spectrometer and quartz cells of 0.1-mm path length. The protein concentration of the purified R fragment was $1.28 \mu\text{M}$ as determined by amino acid analysis in phosphate-buffered saline. Protein samples were hydrolyzed in 6 M HCl at 110°C for 24 h *in vacuo* and subjected to amino acid analysis. The α -helical content was estimated either as described by Bruch *et al.* (22) or using the CONTIN program (23).

Physical Characterization of Recombinantly Expressed CLIP-170 Fragments—The sedimentation coefficient of the purified recombinant proteins was measured by sucrose gradient centrifugation as described before (10). Bacterially expressed proteins purified as described above were dialyzed against PEM, and 0.2-ml samples were loaded onto 4-ml sucrose gradients (5–20% in PEM) and spun at 38,000 rpm for 22 h at 4°C in a TST 60.4 rotor (Kontron, Zurich, Switzerland). Standard proteins and their sedimentation coefficients ($s_{20,w} \times 10^{13}$ S) were bovine heart cytochrome *c* (1.71), bovine serum albumin (4.41), yeast alcohol dehydrogenase (7.40), and sweet potato β -amylase (8.98). Fractions of 0.2 ml were collected from the top of the gradient and analyzed for protein content by a protein assay (24) for the standard proteins and by SDS-PAGE for the recombinant proteins, to locate the peak of undegraded protein; the sucrose concentration was established using a Bausch & Lomb refractometer. The diffusion coefficient, $D_{20,w}$, was measured by gel filtration chromatography on Sephacryl beads. S-300, S-400, and S-500 HR beads (Amersham Pharmacia Biotech) packed in columns of 10-mm diameter by 450-mm length (~ 35 ml total volume) were equilibrated in PEM buffer and run at 0.3 ml/min. Samples of 0.2 ml in PEM were loaded, and 0.6-ml fractions were collected and analyzed by protein assay for standard proteins and by SDS-PAGE for the recombinant proteins. In some cases, the bacterial lysate was analyzed and the protein located by immunoblotting. No significant difference was found between crude and purified proteins. Standard proteins and

their diffusion coefficients ($\times 10^7 \text{ cm}^2/\text{s}$) were bovine heart cytochrome *c* (11.40), chymotrypsinogen A (9.50), chicken ovalbumin (7.03), bovine serum albumin (6.90), sweet potato β -amylase (5.77), bovine γ -globulin (4.10), bovine liver catalase (4.10), horse spleen apoferritin (3.61), bovine thyroglobulin (2.52), and human fibrinogen (1.98). The V_o was measured using the dipeptide Tyr-Gly, and V_o was measured with blue dextran. Not all proteins were resolved on each column; only values that fell on the linear part of a $1/D$ versus K_{av} plot were used, and at least five standard proteins were used to calibrate each column. All standard proteins were purchased from Sigma. The native molecular weight, Stokes radius, axial ratio, and approximate physical dimensions were calculated according to Bloom *et al.* (25).

Analysis of Microtubule Binding—Microtubule binding was assayed as described (10). Briefly, CLIP-170, H1, or H2 were diluted into 50 μl of PEM plus 20 μM paclitaxel and incubated with or without 5 μg of paclitaxel-stabilized microtubules at 37°C for 15 min, before sedimentation through a 100- μl cushion of 10% sucrose in PEM at 30,000 $\times g$ for 30 min at 20°C . The pellet was dissolved in gel loading buffer, and equivalent volumes of the supernatant and pellet samples were separated by 8% SDS-PAGE and staining with Coomassie Blue. For quantitation of proteins in the pellets, serial dilutions of the pellet samples were separated by SDS-PAGE; the Coomassie Blue-stained gels were scanned with an Agfa Arcus II Desktop scanner, and the bands were quantitated using ScanAnalysis version 2.50 software.

Electron Microscopy—Purified protein was equilibrated, either by adding concentrated stock solutions or by dialysis (twice for 1 h against 200 volumes at 4°C), against NMEG. Once in this buffer, the protein samples were either kept on ice for 1 day or snap-frozen in liquid nitrogen and kept at -80°C . Immediately before spraying the samples onto a piece of freshly cleaved mica, more glycerol was added to a final concentration of 30%. Sprayed samples were dried in an evaporator then rotary shadowed at a low elevation angle ($3\text{--}5^\circ$) with platinum/carbon as described (26, 27).

Micrographs were recorded on a Hitachi H-8000 transmission electron microscope (Hitachi Ltd., Tokyo, Japan) operated at 100 kV. For preparing figures, micrographs were digitized with a Leafscan 45 flat-bed scanner (Leaf Systems Inc., Westborough, MA) at a step size of 2450 dpi. The digitized micrographs were processed using Adobe Photoshop (version 5.0) software (Adobe Systems Inc., Mountain View, CA) and printed so that piled up metal (representing molecules) appeared bright on prints. Length measurements of the molecules were performed by computerized tracking on 2.5-fold magnified electron micrographs. The thus-gathered lengths data were presented as histograms that were fitted by Gaussian curves employing the custom-designed IMPSYS program package (28).

RESULTS

Purification and Characterization of Authentic CLIP-170 from Human Placenta—CLIP-170 has previously been isolated from HeLa cells by antibody affinity purification (19). However, the protein obtained was not homogeneous, and the yield was too low to make further purification practical. In order to obtain pure preparations of CLIP-170 in sufficient quantities for further characterization, it was purified to homogeneity from human placenta. Greater quantities of protein might also be obtained by bacterial expression of recombinant CLIP-170, but the complete protein was found to be rapidly degraded in bacteria. However, we expressed and purified recombinant fragments of CLIP-170, which allows characterization of individual functional domains of the protein and comparison of their properties with authentic CLIP-170.

The purification scheme of authentic CLIP-170 from human placenta (Table I) involves affinity chromatography using a mAb against CLIP-170 (19) followed by microtubule affinity purification and gel filtration and is described in detail elsewhere (20). Affinity chromatography using mAb 3A3, the species specificity of which dictated the use of human tissue, was the most effective single purification step, resulting in 5,800-fold enrichment of CLIP-170. The protein is further purified by binding to microtubules, which removes all contaminating proteins to enrich a further 6–7-fold. A final gel filtration step, to remove traces of tubulin introduced in the microtubule-binding step, can be omitted for most biochemical and EM analyses.

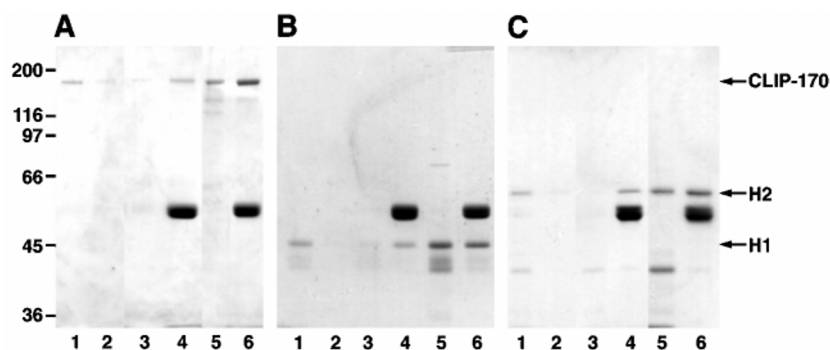


FIG. 3. Analysis of the microtubule-binding activity of placenta CLIP-170 and the bacterial proteins H1 and H2. A, purified human CLIP-170 at ~ 20 (lanes 1–4) or ~ 120 $\mu\text{g/ml}$ (lanes 5 and 6); B, bacterially expressed H1 fragment of CLIP-170 at 50 (lanes 1–4) or 150 $\mu\text{g/ml}$ (lanes 5 and 6); and C, H2 fragment of CLIP-170 at 50 (lanes 1–4) or 150 $\mu\text{g/ml}$ (lanes 5 and 6) were incubated without (lanes 1 and 2) or with (lanes 3–6) paclitaxel microtubules before centrifugation, and supernatants (lanes 1, 3, and 5) and pellets (lanes 2, 4, and 6) were analyzed by 8% SDS-PAGE and staining with Coomassie Blue. Numbers at the left indicate the position of molecular weight markers ($\times 10^{-3}$), and arrows on the right mark the position of CLIP-170, H2, and H1. The structure of H1 and H2 is indicated in Fig. 4. In the absence of microtubules, very little of each protein sediments; there is a higher level of nonspecific pelleting of CLIP-170, most likely due to nonspecific sticking to the tubes. For each protein, the incubation at lower concentration demonstrates that the proteins are fully active for microtubule binding, whereas at higher concentrations a significant proportion remains in the supernatant, showing that the binding is saturable.

TABLE II
Recombinant CLIP-170 fragments expressed in *E. coli*

	H1	H2	H3	R	T1	T2	T3	T4	T5	T6
Sequence from CLIP-170 (amino acids)	1–350	1–481	1–567	425–1238	1237-end	1136-end	1059-end	971-end	828-end	644-end
Polypeptide molecular weight ^a	39,953	55,004	66,426	99,690	20,906	32,314	41,165	51,452	68,118	88,918
Number of amino acids ^a	376	507	608	866	181	282	359	448	589	771
Number of heptad repeats	0	18	25	118	10	25	36	49	69	95
Predicted pI	10.2	7.0	6.9	5.17	4.9	5.1	5.0	5.0	4.9	5.0

^a Molecular weights and total amino acid numbers include the 24 amino acid N-terminal histidine tag and some vector-encoded C-terminal sequence (for H1, H2, H3, and R).

The entire purification scheme yields a 42,000-fold enrichment of CLIP-170 with a yield of 0.2 mg of pure CLIP-170 per 500 g of placenta (Table I). The final product appears homogeneous after gel electrophoresis and silver staining (Fig. 1). By using purified protein as a standard, it was estimated that CLIP-170 represents 0.002% of total placenta high speed supernatant protein.

In order to validate the use of purified CLIP-170 from human placenta for structural studies, we characterized the purified protein and compared it to CLIP-170 from HeLa cells (7, 10, 19). CLIP-170 from HeLa cells and human placenta behave very similarly by SDS-PAGE (see below) or gel filtration chromatography (data not shown), are identical in their reactivity for eight different polyclonal antibodies (seven anti-peptide antibodies and anti-55; Ref. 10) and three different mAbs (2D6, 3A3, 4D3; Ref. 19), and by their behavior during gel filtration chromatography (data not shown). One peptide antibody, anti-KMRL (raised against a peptide according to CLIP-170 amino acids 619–638; see Pierre *et al.* (10)), however, binds to CLIP-170 from HeLa cells but not from human placenta (Fig. 2). This suggests that CLIP-170 from human placenta differs from HeLa CLIP-170 in a small region of the coiled-coil domain. This difference might arise by alternative splicing, similar to what is observed in another CLIP-170 isoform, restin (12, 29).

Proteins co-purifying with CLIP-170 were not detected with the purification scheme used (Fig. 1, lane 4), although binding of CLIP-170 to mAb 3A3 or to microtubules occurred under mild conditions and physiological pH and salt concentrations. Thus, the majority of CLIP-170 appears not to be part of a protein complex or strongly bound to interacting partners, as was previously observed for the protein isolated from HeLa cells. The purification procedure does not significantly alter the shape of CLIP-170, since the purified protein has the same hydrodynamic properties as the protein in the crude lysate

(data not shown). The purified protein was also tested for its ability to bind to paclitaxel-stabilized microtubules. At low concentrations of CLIP-170, most of the protein sediments with the microtubules, but very little sediments in the absence of microtubules (Fig. 3A, cf. lanes 2 and 4). With two different CLIP-170 preparations, it appeared that up to 10% of the protein may be unable to bind to microtubules. This was surprising since it was purified by microtubule affinity; in both cases the protein had been stored frozen before analysis, which may mean there is some loss of activity on freezing. At higher concentrations of CLIP-170, a greater proportion remains in the supernatant, showing that the binding to microtubules is saturable (Fig. 3A, lanes 5 and 6).

Purification and Characterization of Fragments of CLIP-170 Expressed in Bacteria—Previous analysis of the sequence of the cDNA encoding CLIP-170 in HeLa cells predicted three functional domains as follows: an N-terminal 350-amino acid domain, which has been shown to bind to microtubules; a C-terminal 80-amino acid domain, which contains two metal-binding motifs; and a central 960-amino acid domain of heptad repeats (10). To analyze the biochemical and biophysical properties of individual domains of CLIP-170 and to study their structural properties in relation to the authentic protein, various fragments of the protein were expressed from the HeLa cDNA in *E. coli* (summarized in Table II). One series of fragments contains the N-terminal head domain of CLIP-170 with various numbers of heptad repeats from the rod domain (H fragments), another series of fragments contains various numbers of heptad repeats from the rod and the C-terminal tail domain (T fragments), and one fragment (R) consists entirely of the heptad repeats of the central rod domain (Fig. 4A). The proteins were expressed with N-terminal histidine tags and purified for analysis. All the expressed fragments had the expected size as determined by gel electrophoresis (Fig. 4B) and

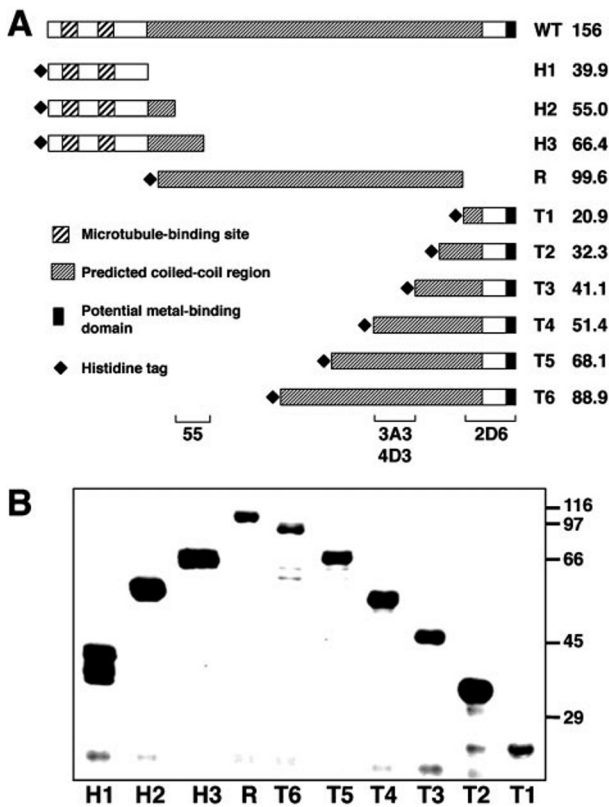


FIG. 4. Expression of CLIP-170 fragments as fusion proteins in bacteria. *A*, the primary structure of fragments of CLIP-170 expressed in bacteria is schematized and compared with that of CLIP-170 (wild type, WT). The name of each protein and the predicted molecular weight of the polypeptide ($\times 10^{-3}$) is indicated on the right. At the bottom is indicated the regions containing the epitopes recognized by four antibodies against CLIP-170. *B*, the recombinant fragments of CLIP-170 expressed in bacteria and purified were separated on 12% SDS gels and stained with Coomassie Blue. Names of the proteins are those given in *A*, and numbers at the right indicate the position of molecular weight markers ($\times 10^{-3}$).

immunoblotting with anti-peptide antibodies (data not shown).

The shape and state of oligomerization of CLIP-170 fragments were determined by calculating their native molecular weights and dimensions, based on measurements of diffusion coefficients and sedimentation coefficients of the recombinant fragments. This analysis indicates that all are elongated molecules with widths of less than 5 nm (summarized in Table III). Calculation of the native molecular weight of the fragments shows that proteins that do not contain heptad repeats of the rod domain (H1) are monomeric, whereas proteins that contain heptad repeats (H2, 18 heptads) are dimeric. All of the expressed T constructs are also dimeric, including T1 that contains only 10 heptad repeats. This suggests that both the beginning and end of the coiled-coil domain have a strong tendency to associate to form dimeric structures. All of the dimeric H and T constructs are much longer than predicted for their coiled-coil regions (30), suggesting that both the N- and C-terminal domains of CLIP-170 are rather elongated. The N-terminal domain appears to be 35–50 nm long, and the C terminus ~15 nm long. This is confirmed for the N-terminal domain by measurement of the monomeric H1, which has a measured length of 35 nm (Table III). The central domain, which consists entirely of 116 heptad repeats, is a thin rod with estimated dimensions of 116×2 nm. Circular dichroism measurements, revealing characteristic minima at 208 and 222 nm (Fig. 5), confirm the α -helical nature of the rod domain. The percentage of α -helical content was estimated by two different

methods (22, 23) to be between 91 and 97%. The length of the rod domain (116 nm) and its α -helical nature are in agreement with the presence of 116 heptad repeats with a predicted length of ~1 nm each in coiled-coils (30).

Previous work has shown that the N-terminal 350-amino acid fragment of CLIP-170 (H1) contains the microtubule-binding domain (10). The availability of highly purified authentic protein and fragments thereof enables quantitative analysis of their microtubule-binding properties. In addition, comparison of monomeric H1 with dimeric H2 and authentic protein allows determination of the effect of dimerization of rod and tail domains on microtubule binding. Both H1 and H2 did not sediment in the absence of microtubules, were fully active in binding to microtubules, and the binding was saturable (Fig. 3, *B* and *C*). The stoichiometry of binding of CLIP-170, H1, and H2 to microtubules was estimated by quantitative scanning of gels of the pellet samples at saturation (Fig. 3, *A–C*, lane 6). Weight ratios of tubulin to CLIP-170, H1, and H2 were 4.5:1, 4.4:1, and 3.9:1 respectively. By using molecular weights of 100,000 for tubulin (31), 306,000 for CLIP-170 (10), 40,000 for H1, and 110,000 for H2 (Table III), these values give molar ratios of tubulin:protein of 13.8:1, 1.8:1 and 4.3:1, for CLIP-170, H1, and H2, respectively. Thus, the rod domain or the C-terminal domain negatively influences the binding of CLIP-170 to microtubules, which might be due to structural properties of these domains.

EM Analysis of Authentic CLIP-170 and Recombinantly Expressed Fragments—EM after glycerol spraying/low angle rotary metal shadowing of the samples was used to visualize directly the authentic and recombinant proteins. Authentic CLIP-170 yielded long, often bent or kinked, rod-shaped particles (Fig. 6*a*). Frequently one or sometimes both ends of these rod-shaped molecules were flanked by a pair of small globular heads, which had some tendency to coalesce. However, the variability of the two end domains from one particle to the next was such that no clear polarity of the CLIP-170 molecule became apparent. This morphological finding was somewhat surprising since the two end domains were expected to be rather asymmetric (*i.e.* the N-terminal end domain is 350 whereas the C-terminal end domain is 80 amino acid residues long). Nevertheless, it is likely that the N-terminal end domain of the purified protein is folded correctly, since it binds to microtubules, an activity mediated by the N-terminal end domain.

The average length of the central rod domain of CLIP-170 seen by EM of glycerol-sprayed/low angle rotary metal-shadowed samples was measured to be 135 nm (Fig. 6), in good agreement with the predicted length of a 959-residue-long (residues 350–1308) two-stranded α -helical coiled-coil (*i.e.* ~140 nm). This value is also consistent with the length previously calculated from biophysical properties of CLIP-170 from HeLa cells (*i.e.* 110 nm) (10). Hence, the overall size and shape of the full-length human CLIP-170 molecule as determined by EM fits best with a rod-shaped homodimer with two polypeptides being associated in register via their central 959-residue-long, heptad repeat-containing rod domain to form a 2-stranded α -helical coiled-coil.

The bacterially expressed fragments of CLIP-170 were also analyzed by EM of glycerol-sprayed/rotary metal-shadowed samples. None of the three C-terminal truncation constructs (H1, H2, and H3; see Table II) appeared as rod-shaped particles (shown for H3 in Fig. 6*b*). This is predicted for the H1 fragment, which lacks heptad repeats (Table II) and stays monomeric according to biophysical measurements (Table III). However, the finding is somewhat surprising for the H2 and H3 constructs, which contain 18 and 30 heptad repeats, respectively (see Table II), and, upon dimerization via 2-stranded α -helical

TABLE III
Physical measurements of CLIP-170 fragments

	H1	H2	R	T1	T2	T5
Measured properties						
Sedimentation coefficient, $s_{20,w}$ ($\times 10^{13}$) ^a	2.13 \pm 0.25 (<i>n</i> = 3)	3.50 \pm 0.33 (<i>n</i> = 3)	3.79 \pm 0.07 (<i>n</i> = 3)	2.91 \pm 0.06 (<i>n</i> = 3)	3.02 \pm 0.03 (<i>n</i> = 3)	3.59 \pm 0.27 (<i>n</i> = 3)
Diffusion coefficient, $D_{20,w}$ ($\times 10^7$ cm ² /s) ^a	4.72 \pm 0.40 (<i>n</i> = 6)	2.81 \pm 0.47 (<i>n</i> = 6)	1.77 \pm 0.07 (<i>n</i> = 5)	5.59 \pm 0.22 (<i>n</i> = 5)	3.60 \pm 0.36 (<i>n</i> = 5)	2.25 \pm 0.15 (<i>n</i> = 5)
Calculated properties						
Native molecular weight	40,000	110,000	189,000	46,000	74,000	141,000
Number of subunits	1	2	2	2	2	2
Axial ratio	22	32	60	11	24	43
Estimated dimensions (nm)	1.6 by 35	2.0 by 64	1.9 by 116	2.0 by 23	2.0 by 46	2.0 by 84
Stokes radius (nm)	4.5	7.6	12.1	3.8	5.9	9.5

^a Values are \pm S.E. (*n* = number of measurements).

DISCUSSION

CLIP-170 is a cytoplasmic linker protein proposed to mediate transient interactions of organelles with microtubules (10, 11). We have analyzed purified authentic CLIP-170 and bacterially expressed fragments to elucidate the organization and structure of the functional domains of the protein. EM analysis of glycerol-sprayed/rotary metal-shadowed protein revealed the elongated structure of CLIP-170, but the lack of difference in morphology between the two ends of the authentic molecule does not by itself allow any conclusion about the parallel or antiparallel orientation of the two subunits. However, the efficient dimerization of the recombinant H2 and T1 fragments suggests that these domains are oriented in parallel in the authentic protein. In addition, in the case of the N-terminal deletions, a kink \sim 37 nm from the C-terminal end is identically placed to that seen in the authentic protein. Taken together, these data clearly indicate that the two subunits within the authentic CLIP-170 molecule are oriented in a parallel, unstaggered fashion. Structural analysis of kinesin, a motor protein, has also revealed a polar molecule with a distinct tripartite structure consisting of an N-terminal microtubule-binding motor domain, a central rod domain harboring a kink (32–34), and a C-terminal end domain most likely interacting with membranes (35). This domain organization is consistent with the function of motor proteins or CLIPs of linking cargo molecules or organelles to microtubules.

The recombinant N-terminal domains of CLIP-170 purified after expression in bacteria appear to be elongated based on biophysical measurements, but they did not reveal a distinct particle morphology by EM analysis despite the presence of \leq 30 heptad repeats in these truncation constructs. This may indicate that the N-terminal \geq 30 heptad repeats are lacking a coiled-coil “trigger” sequence which, in turn, is absolutely necessary for stable α -helical coiled-coil formation (36, 37). Hence, the dimerization observed for the H2 and H3 fragments by physical measurements may occur by a different mechanism, potentially yielding only short, out-of-register coiled-coil segments that are not stable enough to withstand the mechanical shear and stress occurring during specimen preparation (*i.e.* spraying, adsorption, and dehydration) for EM analysis. In contrast, fragments T5 and T6 examined by EM appeared consistent with the authentic protein and indeed contain a coiled-coil trigger sequence identified within the central rod domain of CLIP-170 (37).

Authentic CLIP-170 analyzed by EM frequently exhibited globular domains at both ends, whereas the recombinant N-terminal domain (H1) purified after expression in bacteria appears to be elongated based on biophysical measurements. A relatively unfolded structure for this domain may account for its lack of structural stability by EM analysis, leading to a globular appearance. It is unlikely that this domain was dena-

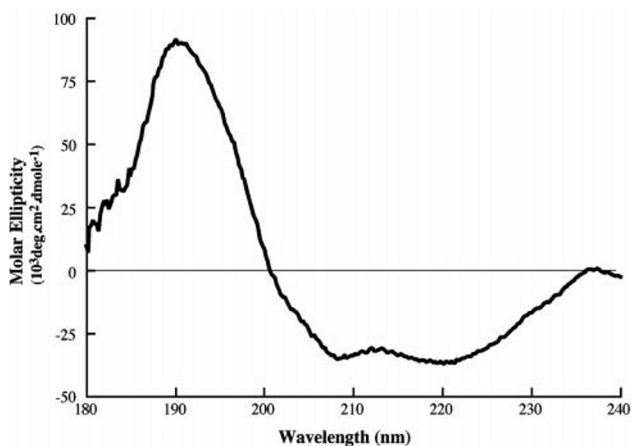


FIG. 5. Far ultraviolet circular dichroism spectrum of the R fragment. Ellipticities are expressed per mol of peptide bonds.

coiled-coil formation, should yield rod-shaped segments \sim 20 and $>$ 30 nm long, respectively. In contrast, the three C-terminal constructs (T3, T5, and T6; see Table II) yielded rod-shaped particles (Fig. 6, *c–e*) with average lengths (Fig. 6, length histograms) which agree with the size predicted from their corresponding α -helical coiled-coil rod segments (Table II).

Since the EM images of both the authentic and N-terminally truncated CLIP-170 frequently revealed one or two distinct kinks (Fig. 6, *a* and *c*), we analyzed statistically the distances of these kinks from the termini of the protein and from each other (Fig. 7). Whereas in the case of the full-length authentic protein, due to the lack of evident polarity, the assignment of their N- and C-terminal end was arbitrary, in the case of the N-terminally truncated CLIP-170 fragments, T6 and T5, we could in most cases morphologically determine their C-terminal ends. In the case of full-length CLIP-170, the two kinks were rather symmetrically spaced from the particle ends, for example 36 ± 10 nm from one end and 38 ± 11 nm from the other end (Fig. 7), with the two kinks being spatially separated by 63 ± 12 nm. Analysis of the N-terminally truncated fragments T5 and T6 shows that the kink is 36 ± 4 or 37 ± 6 nm from the C terminus, respectively (Fig. 7). A 36-nm-long coiled-coil rod segment corresponds to \sim 34 heptad repeats (30), *i.e.* 250 amino acids, and analysis of the CLIP-170 sequence by the *PairCoil* program suggests that the coiled-coil domain covers residues 350–1300. The N-terminal kink should, therefore, occur around amino acid residue 600 ($350 + 250$), whereas the C-terminal kink should occur around amino acid residue 1050 ($1300 - 250$). Indeed, an interruption of the heptad-repeat pattern in the primary sequence is predicted around residue 600 but not around residue 1050.

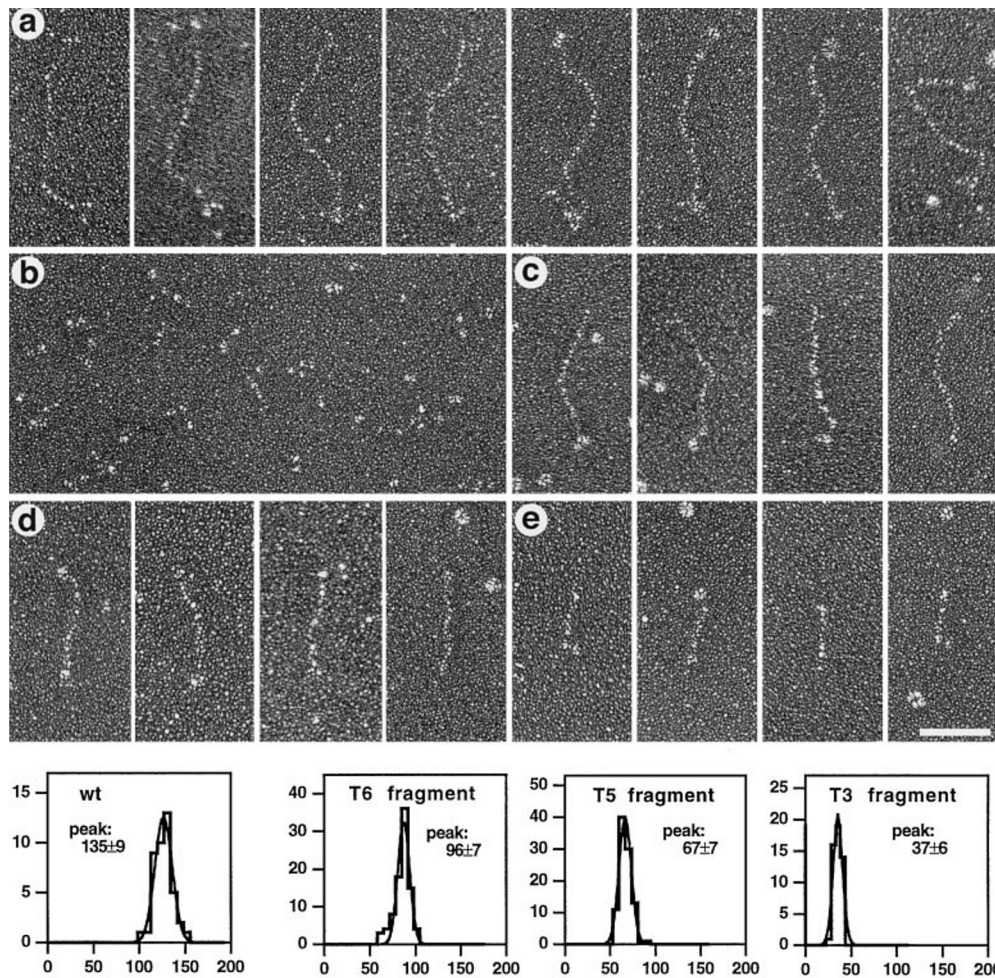


FIG. 6. **Electron microscopic analysis of human CLIP-170 and recombinantly expressed CLIP-170 fragments.** Selected particle galleries of human CLIP-170 (a), of a C-terminally truncated fragment H3 (b), and of N-terminally truncated fragments T6 (c), T5 (d), and T3 (e) after preparation of the samples by glycerol spraying/low angle rotary metal shadowing. *Bottom*, length histograms measured from authentic and recombinant CLIP-170 particles displayed in (a–e). Particle length in nanometers on the *abscissa* is plotted against the number of particles on the *ordinate*. The histograms were fitted by a single Gaussian curve to give the mean length in nanometers (\pm S.D.). *Scale bar*, 50 nm (a–e).

tured in our purified proteins, since they can still bind to microtubules, and we have shown that purified H2 behaves like authentic CLIP-170 in promoting microtubule assembly and binding preferentially to polymerizing microtubule ends (8). H2 thus appears to be a good model protein for the study of the microtubule binding properties of CLIP-170, and comparison of purified monomeric and dimeric head domains of CLIP-170 will be useful in future studies of the effect of dimerization on its interaction with microtubules. Thus, the microtubule-binding domain of CLIP-170 may be an elongated structure, although we cannot exclude the possibility that the actual microtubule-binding moiety of CLIP-170 is indeed folded into a small globular domain and that it is the presence of an “extended neck” that gives rise to the predicted elongated form of H1 based on biophysical measurements. In contrast, the microtubule-binding domain of kinesin is globular (33, 34), and the microtubule-binding domain of dynein has also been shown to consist of a globular structure, although found at the tip of an elongated stalk (38). On the other hand, the microtubule-binding repeat region of tau also appears to be rather elongated (39); this elongated structure may therefore be a characteristic of MBPs, as opposed to motor proteins that display cyclic binding to microtubules during translocation.

We observed two kinks in the rod domain of CLIP-170, each ~ 37 nm from the corresponding end. These kinks may add

mechanical flexibility to the long, relatively stiff rod domain which, in turn, may be of functional significance, for example, to optimize sterically the binding of CLIP-170 to microtubules and/or vesicles. The rod domain of kinesin, which appears to be less stable than that of CLIP-170 based on its α -helical content, contains one kink which might be involved in regulating kinesin activity by folding back of the C-terminal end domain onto the N-terminal half of its rod domain (40, 41). Similarly, myosin can undergo a phosphorylation-induced conformational transition that regulates filament assembly (42–44). The kinks in the rod domain of CLIP-170 might similarly regulate the function of this protein as a microtubule-organelle linker (see below). In this respect, it is interesting that alternatively spliced isoforms of CLIP-170 exist; a human isoform with a 35-amino acid insert in the rod domain has been termed restin (29), and both these isoforms, as well as two others, have been identified in chicken and human (12, 45). The isoforms are coexpressed in several tissues, but there are tissue-specific differences in their expression levels (12, 45). We found that the protein purified from human placenta did not react with an antibody raised against amino acids 619–638 of HeLa CLIP-170, a sequence also present in restin and other identified isoforms (12, 45), suggesting that this represents a further isoform that is the form predominantly expressed in human placenta. Unlike the identified alternatively spliced inserts,

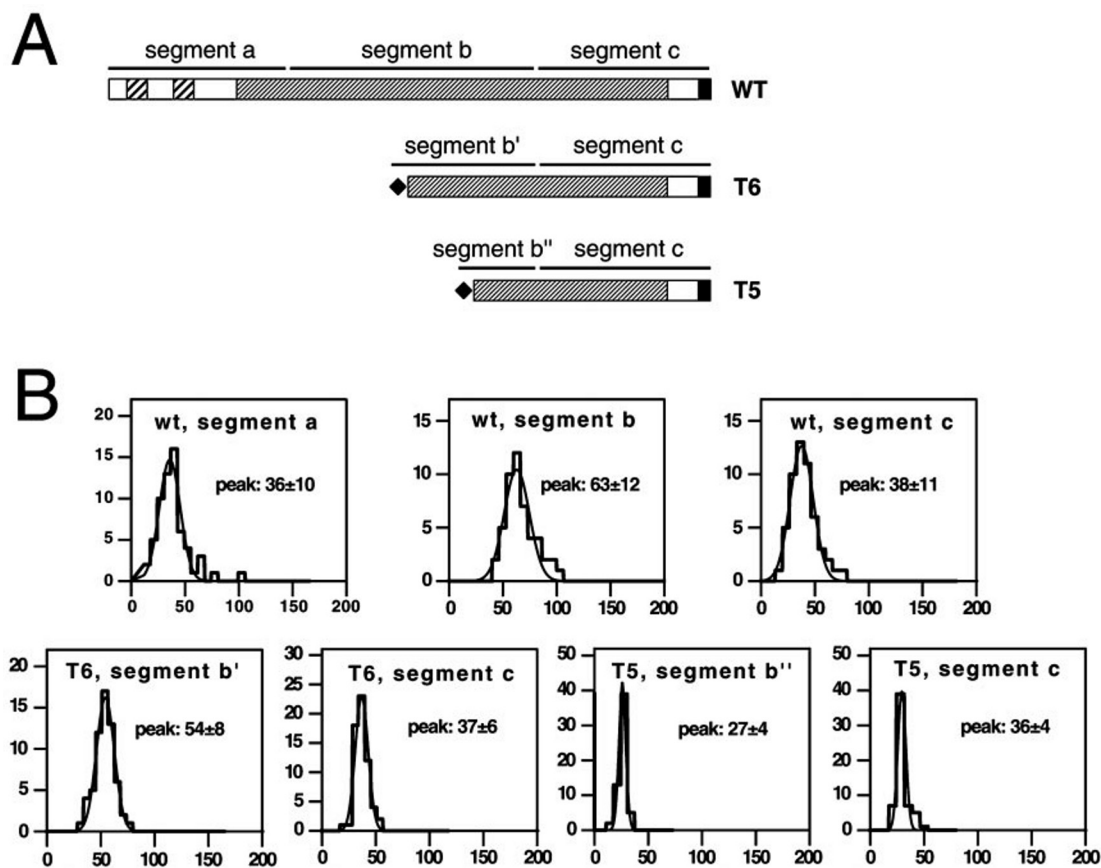


FIG. 7. Analysis of the position of kinks in the rod domain of CLIP-170. Statistical analysis of the positions of two distinct kinks detected in the rod domain of CLIP-170 (*wt*) and the N-terminally truncated fragments T6 and T5. *A*, schematic representation of the molecules showing the particle segments measured: *a*, distance of the N-terminal kink to the N terminus; *c*, distance of the C-terminal kink to the C terminus; *b*, distance between the two kinks; *b'* and *b''*, distance of the C-terminal kink to the N terminus of T6 and T5, respectively. *B*, particle length in nanometers on the *abscissa* is plotted against number of particles on the *ordinate*. The histograms were fitted by a single Gaussian curve to give the mean length in nanometers (\pm S.D.). Assignment of the N and C termini of the full-length CLIP-170 molecule was arbitrary.

which are completely conserved between human and chicken (12, 45), this region is not as well conserved between the two species (45% identity over 20 amino acids).

Our results suggest that the H1 monomer saturates the microtubule at two tubulin heterodimers, whereas the H2 dimer saturates it at four tubulin heterodimers. This would be consistent with binding of one CLIP-170 head domain to two tubulin heterodimers and independent and equivalent binding of each head domain in the CLIP-170 dimer. In contrast, the molar stoichiometry we obtained for the binding of authentic CLIP-170 to microtubules is much lower. It is possible that we did not in fact achieve saturation of the microtubules in this experiment; the large amount of protein required for this experiment made it impractical to use more. However, it is conceivable that the \sim 120-nm-long rod domain of the authentic protein causes problems of steric hindrance. As proposed above, this steric hindrance could be reduced by introducing kinks into the long, relatively stiff rod domain, thereby providing a mechanism, ¹in addition to phosphorylation (19), to regulate (or optimize) the interaction of CLIP-170 with microtubules. We indeed have evidence that CLIP-170 and MAP2, both elongated proteins, interfere with the binding of each other to microtubules, although they do not compete for the same site on tubulin,² and heat-stable MAPs also inhibit binding of endocytotic organelles to microtubules mediated by CLIP-170 (46). Therefore, steric effects rather than number of binding sites may limit the binding of large proteins to microtubules. Consistent

with this, the stoichiometry of binding of several large, asymmetric MAPs, MAP2, MAP1A, and XMAP, has been measured as 8–9:1, 13–15:1, and 16:1, respectively (47, 48), whereas that for the lower molecular weight, more globular tau is 2:1 (39), although MAP2 and tau contain homologous microtubule-binding domains.

The microtubule-binding motifs in the N-terminal domain of CLIP-170 are also found in a number of other proteins (for summary see Ref. 6), of which the best characterized is dp150^{glued}, a subunit of the dynactin complex. The homology is in the N-terminal domain of dp150^{glued}, which extends from the dynactin complex and appears to be globular (49). We found the N terminus of CLIP-170 to be rather elongated according to biophysical measurements, although by EM a pair of small globular heads was often detected at either end of the molecule. This difference might be due to the different techniques used to prepare the proteins for EM or might be caused by the presence of p24 or p27 bound to this domain of dp150^{glued}, but one difference at the level of the primary structure is the presence of two copies of the microtubule-binding motif in CLIP-170 compared with only one in dp150^{glued}. One of the repeats is sufficient to allow binding of CLIP-170 to microtubules (10), and the dp150^{glued} polypeptide can bind to microtubules *in vitro* and *in vivo* (50). However, since each of the repeats in CLIP-170 is alone able to mediate microtubule binding (10, 21), an elongated structure for the authentic CLIP-170 head domain may be necessary to allow both these sequences to function in interacting with the elongated tubulin polymer. Interaction of each of these motifs with one subunit of the polymer

² G. S. Diamantopoulos, unpublished observations.

would also be consistent with the stoichiometry of microtubule binding measured for the H1 and H2 proteins.

From the analysis reported here, we conclude that CLIP-170 is an elongated molecule formed by parallel homodimerization via a coiled-coil structure. This separates the microtubule-binding domain from the opposite end, which interacts with other organelles (11). This head-to-tail domain organization has also been noted for the microtubule- and actin-based motor proteins (51) and appears to be a common mechanism for organization of proteins that link an organelle to the cytoskeleton. The more elongated structure of the microtubule-binding domain of CLIP-170 compared with kinesin would be consistent with a microtubule-stabilizing function of CLIP-170, which could have the cellular role of allowing transient interactions with organelles to lead to polarization and stabilization of the cytoskeleton.

Acknowledgments—We thank B. Schwendimann for performing the amino acid analysis of the R fragment. We are grateful to the Lausanne abattoir for provision of pig brains and to the staff of the Maternity Hospital, Hôpital Université de Genève, for help in obtaining placentas. We also thank the NCI, National Institutes of Health (Bethesda), for gifts of paclitaxel.

REFERENCES

- Kirschner, M., and Mitchison, T. (1986) *Cell* **45**, 329–342
- Rickard, J. E., and Kreis, T. E. (1996) *Trends Cell Biol.* **6**, 178–183
- Goodson, H. V., Valetti, C., and Kreis, T. E. (1997) *Curr. Opin. Cell Biol.* **9**, 18–28
- Schroer, T. A., Bingham, J. B., and Gill, S. R. (1996) *Trends Cell Biol.* **6**, 212–215
- Vallee, R. B., and Sheetz, M. P. (1996) *Science* **271**, 1539–1544
- Rickard, J. E. (1999) in *Guidebook to the Cytoskeletal and Motor Proteins* (Kreis, T. E., and Vale, R. D., eds) 2nd Ed., Oxford University Press, Oxford
- Rickard, J. E., and Kreis, T. E. (1990) *J. Cell Biol.* **110**, 1623–1633
- Diamantopoulos, G. S., Perez, F., Goodson, H. V., Batelier, G., Melki, R., Kreis, T. E., and Rickard, J. E. (1999) *J. Cell Biol.* **144**, 99–112
- Perez, F., Diamantopoulos, G. S., Stalder, R., and Kreis, T. E. (1999) *Cell* **96**, 517–527
- Pierre, P., Scheel, J., Rickard, J. E., and Kreis, T. E. (1992) *Cell* **70**, 887–900
- Dujardin, D., Wacker, U. I., Moreau, A., Schroer, T. A., Rickard, J. E., and De Mey, J. R. (1998) *J. Cell Biol.* **141**, 849–862
- Griparic, L., Volosky, J. M., and Keller, T. C. S., III (1998) *Gene (Amst.)* **206**, 195–208
- Lantz, V. A., and Miller, K. G. (1998) *J. Cell Biol.* **140**, 897–910
- Holzbaur, E. L. F., Hammarback, J. A., Paschal, B. M., Kravit, N. G., Pfister, K. K., and Vallee, R. B. (1991) *Nature* **351**, 579–583
- Swaroop, A., Swaroop, M., and Garen, A. (1987) *Proc. Natl. Acad. Sci. U. S. A.* **84**, 6501–6505
- Trueheart, J., Boeke, J. D., and Fink, G. (1987) *Mol. Cell. Biol.* **7**, 2316–2328
- Tian, G., Huang, Y., Rommelaere, H., Vandekerckhove, J., Ampe, C., and Cowan, N. J. (1996) *Cell* **86**, 287–296
- Tian, G., Lewis, S. A., Feierbach, B., Stearns, T., Rommelaere, H., Ampe, C., and Cowan, N. J. (1997) *J. Cell Biol.* **138**, 821–832
- Rickard, J. E., and Kreis, T. E. (1991) *J. Biol. Chem.* **266**, 17597–17605
- Diamantopoulos, G. S., Scheel, J., Kreis, T. E., and Rickard, J. E. (1998) *Methods Enzymol.* **298**, 197–206
- Pierre, P., Pepperkok, R., and Kreis, T. E. (1994) *J. Cell Sci.* **107**, 1909–1920
- Bruch, M. D., Dhingra, M. M., and Gierach, L. M. (1991) *Proteins* **10**, 130–139
- Provencher, S. W., and Glöckner, J. (1981) *Biochemistry* **20**, 33–37
- Bradford, M. M. (1976) *Anal. Biochem.* **72**, 248–254
- Bloom, G. S., Wagner, M. C., Pfister, K. K., and Brady, S. T. (1988) *Biochemistry* **27**, 3409–3416
- Fowler, W. E., and Aebi, U. (1983) *J. Ultrastruct. Res.* **83**, 319–334
- Häner, M., Bremer, A., and Aebi, U. (1997) in *Cell Biology: A Laboratory Handbook* (Celis, J. E., ed) pp. 292–298, Academic Press, San Diego
- Müller, S. A., Goldie, K. N., Bürki, R., Häring, R., and Engel, A. (1992) *Ultramicroscopy* **46**, 317–334
- Bilbe, G., Delabie, J., Brügggen, J., Richener, H., Asselbergs, F. A. M., Cerletti, N., Sorg, C., Odink, K., Tarcsay, L., Wiesendanger, W., DeWolf-Peters, C., and Shipman, R. (1992) *EMBO J.* **11**, 2103–2113
- Bourne, H. R. (1991) *Nature* **351**, 188–190
- Mandelkow, E.-M., and Mandelkow, E. (1993) in *Guidebook to the Cytoskeletal and Motor Proteins* (Kreis, T. and Vale, R., eds) 1st Ed., pp. 127–130, Oxford University Press, Oxford
- Amos, L. (1987) *J. Cell Sci.* **87**, 105–111
- Hirokawa, N., Pfister, K. K., Yorifuji, H., Wagner, M. C., Brady, S. T., and Bloom, G. S. (1989) *Cell* **56**, 867–878
- Scholey, J. M., Heuser, J., Yang, J. T., and Goldstein, L. S. B. (1989) *Nature* **338**, 355–357
- Skoufias, D. A., Cole, D. G., Wedaman, K. P., and Scholey, J. M. (1994) *J. Biol. Chem.* **269**, 1477–1485
- Steinmetz, M. O., Stock, A., Schulthess, T., Landwehr, R., Lustig, A., Faix, J., Gerisch, G., Aebi, U., and Kammerer, R. A. (1998) *EMBO J.* **17**, 1883–1891
- Kammerer, R. A., Schulthess, T., Landwehr, R., Lustig, A., Aebi, U., and Steinmetz, M. O. (1998) *Proc. Natl. Acad. Sci. U. S. A.* **95**, 13419–13424
- Gee, M. A., Heuser, J. E., and Vallee, R. B. (1997) *Nature* **390**, 636–639
- Wille, H., Drewes, G., Biernat, J., Mandelkow, E.-M., and Mandelkow, E. (1992) *J. Cell Biol.* **118**, 573–584
- Hisanaga, S., Murofushi, H., Okuhara, K., Sato, R., Masuda, Y., Sakai, H., and Hirokawa, N. (1989) *Cell Motil. Cytoskel.* **12**, 264–272
- Hackney, D. D., Levitt, J. D., and Suhan, J. (1992) *J. Biol. Chem.* **267**, 8696–8701
- Suzuki, H., Kamata, T., Onishi, H., and Watanabe, S. (1982) *J. Biochem. (Tokyo)* **91**, 1699–1705
- Trybus, K. M., Huiatt, T. W., and Lowey, S. (1982) *Proc. Natl. Acad. Sci. U. S. A.* **79**, 6151–6155
- Craig, R., Smith, R., and Kendrick-Jones, J. (1983) *Nature* **302**, 436–439
- Griparic, L., and Keller, T. C. S., III (1998) *Biochim. Biophys. Acta* **1405**, 35–46
- Scheel, J., and Kreis, T. E. (1991) *J. Biol. Chem.* **266**, 18141–18148
- Pedrotti, B., and Islam, K. (1994) *Biochemistry* **33**, 12463–12470
- Gard, D. W., and Kirschner, M. W. (1987) *J. Cell Biol.* **105**, 2203–2215
- Schafer, D. A., Gill, S. R., Cooper, J. A., Heuser, J. E., and Schroer, T. A. (1994) *J. Cell Biol.* **126**, 403–412
- Waterman-Storer, C. M., Karki, S., and Holzbaur, E. L. (1995) *Proc. Natl. Acad. Sci. U. S. A.* **92**, 1634–1638
- Schliwa, M. (1989) *Cell* **56**, 719–720